EVAPORATIVE COOLING OF FLARE PLASMA

by

S.K. Antiochos and P.A. Sturrock

National Aeronautics and Space Administration

Grant NGL 05-020-272

Office of Naval Research

Contract N00014-75-C-0673

SUIPR Report No. 676

November 1976

INSTITUTE FOR PLASMA RESEARCH
STANFORD UNIVERSITY, STANFORD, CALIFORNIA

EVAPORATIVE COOLING OF FLARE PLASMA

by

S.K. Antiochos* and P.A. Sturrock*

National Aeronautics and Space Administration

Grant NGL 05-020-272

Office of Naval Research

Contract N00014-75-C-0673

SUIPR Report No. 676

November 1976

Institute for Plasma Research
Stanford University
Stanford, California

*Also Department of Applied Physics

EVAPORATIVE COOLING OF FLARE PLASMA

by

S.K. Antiochos and P.A. Sturrock
Institute for Plasma Research
and
Department of Applied Physics
Stanford University
Stanford, California

ABSTRACT

We investigate a one-dimensional loop model for the evaporative cooling of the coronal flare plasma. The important assumptions are that conductive losses dominate radiative cooling and that the evaporative velocities are small compared to the sound speed. We calculate the profile and evolution of the temperature and verify that our assumptions are accurate for plasma parameters typical of flare regions. The model is in agreement with soft x-ray observations on the evolution of flare temperatures and emission measures. The effect of evaporation is to greatly reduce the conductive heat flux into the chromosphere and to enhance the EUV emission from the coronal flare plasma.

I. Introduction

It is becoming widely accepted that flares evaporate large masses of chromospheric material into the corona. The most compelling arguments for the occurrence of this process come from soft x-ray observations. Measurements of the emission measure, which appear to be well over 10^{50} cm^{-3} for some flares (Phillips and Neupert, 1973), indicate a total mass of hot ($T \geq 10^7$ K) plasma in the corona as large as 10^{16} g. Similar mass estimates are obtained from loop prominence systems which are known to occur in post-flare regions (Jefferies and Orrall, 1965). This amount of plasma is too large to condense from the corona and must somehow be extracted from the chromosphere.

Neupert (1968) was perhaps the first to realize that corona flare plasma is the result of evaporation from the chromosphere. Similar ideas were expressed subsequently by Hudson and Ohki (1972) and by Sturrock (1973). In these papers, it was implicitly assumed that evaporation occurs during the initial deposition of energy into the chromosphere by means of high-energy electron streams. However, there appears to be observational evidence for evaporation during the decay phase of flares. The emission measure is often seen to increase while the total thermal energy does not increase and the temperature decreases (Kahler et al., 1970; Horan, 1971). "Moving boundary" types of models have been proposed, to explain these results, by Strauss and Papagiannis (1971) and by Zauman and Acton (1974). These models involve the assumption that flare heating occurs only at the top of a loop of coronal plasma, which results in an expanding hot region. The loop is assumed to be essentially infinite in length so that the effect of the heating on

the chromosphere is not included. However, these models encounter certain difficulties: in particular, they cannot account for the origin of the large masses required by the soft x-ray observations. Furthermore, if the "moving boundary" models were correct, flares should heat the corona well before they heat the chromosphere, whereas observations indicate that the Hα emission of flares begins well before the soft x-ray maximum. We therefore take the view that the increase of emission measure during the decay phase of a flare indicates that evaporation occurs not only during the impulsive phase of a flare but also during the decay phase.

From the above considerations, it appears that there may be two evaporation mechanisms occurring during a solar flare. One is associated with the direct heating of the chromosphere by the energy released during the impulsive phase of a flare, the energy probably being transferred by an electron stream. This stage is likely to involve large pressure gradients and large velocities, quite possibly leading to shock waves. It seems likely that a separate evaporation process may occur after the primary energy release is finished, this evaporation being driven by the large conductive heat flux from the high-temperature flare plasma contained in magnetic flux tubes above the chromosphere. In this stage, evaporation is a cooling process competing with radiation. It seems likely that energy loss by evaporation dominates early in the decay phase, and energy loss by radiation dominates later, when the density of flare plasma is higher and the temperature is lower. Moreover, it seems likely that this evaporation stage would involve only small pressure gradients and velocities. It is this later, "gentle", evaporation process which we discuss in this article.

II. Model

Since the magnetic field strength in typical post-flare regions appears to be large ($B \geq 10$ g, Rust and Bar, 1973), we assume that it dominates the plasma so that mass flow and heat transfer are both parallel to the magnetic field. The geometry which we adopt is that of a flare loop consisting of a narrow current-free flux tube with the independent variable s measuring distance along the loop (parallel to $\vec{B}$) from the top of the loop. The cross-sectional area of the flux tube is given by $A(s)$ and will depend on the form of the magnetic field. The field is assumed to be that of a point-dipole or of a line-dipole, but we also calculate the case of a loop of constant cross section corresponding approximately to the familiar plane-parallel model.

We make two assumptions on the state of the plasma. The first is that radiation losses are negligible. We later check our assumption by comparing the radiative cooling time with the conductive cooling time to be derived below.

Our second assumption is that the velocities generated by the evaporation process are small compared with the speed of sound. Since the temperature is high enough that gravitational effects are negligible (i.e., the scale height is large compared with the size of the flux tube), this assumption is equivalent to setting

$$\frac{\partial p}{\partial s} \simeq 0 \quad . \tag{2.1}$$

At this point it may seem paradoxical that we can calculate the plasma velocities by neglecting the pressure gradients, since these gradients create the velocities in the first place. However, one

finds that, if the gravitational term is negligible, the fractional variation of pressure along the flux tube is of order M^2, where the Mach number M is given by

$$M = v/C \quad , \tag{2.2}$$

where C is the speed of sound. Hence our assumption (2.1) is equivalent to the assumption that $M \ll 1$, which must be verified a posteriori.

Equation (2.1) shows that the pressure is independent of s. We assume that there is no heat input into the loop, and we ignore radiation. Hence the total energy in the loop is constant, which implies that the pressure is also independent of time:

$$p(s,t) = \text{const.} \tag{2.3}$$

On using equation (2.2), one finds that the energy equation may be expressed as

$$-\frac{5}{2}\frac{p}{\rho}\left(\frac{\partial \rho}{\partial t} + v\frac{\partial \rho}{\partial s}\right) = \frac{1}{A}\frac{\partial}{\partial s}\left(A\kappa\frac{\partial T}{\partial s}\right) \quad . \tag{2.4}$$

On combining equation (2.4) with the continuity equation

$$\frac{\partial \rho}{\partial t} + \frac{1}{A}\frac{\partial}{\partial s}(A\rho v) = 0 \quad , \tag{2.5}$$

we obtain

$$\frac{\partial}{\partial s}\left[A\left(\frac{5}{2}pv - \kappa\frac{\partial T}{\partial s}\right)\right] = 0 \quad . \tag{2.6}$$

We see from (2.6) that

$$A\left(\frac{5}{2}pv - \kappa\frac{\partial T}{\partial s}\right) = f(t) \quad . \tag{2.7}$$

The temperature of the chromosphere (the base of our model) is sufficiently low that the heat flux F, given by

$$F = -\kappa \frac{\partial T}{\partial s} \quad , \tag{2.8}$$

may be neglected. Similarly, the density there is so high that the mass velocity v may be neglected. These boundary conditions thus lead to the simple relation

$$v = \frac{2}{5} \frac{\kappa}{p} \frac{\partial T}{\partial s} \quad , \tag{2.9}$$

which may alternatively be expressed as

$$F = -\frac{5}{2} pv \quad . \tag{2.10}$$

Equation (2.10) can also be obtained from the symmetry of the loop since if the loop is symmetric about the top, it follows that F and v must vanish there.

The heat equation may now be expressed with only temperature as dependent variable. On replacing v in equation (2.4) by the expression (2.9), and then eliminating ρ in favor of T by means of the equation of state, we obtain

$$\frac{5}{2} \frac{p}{T} \frac{\partial T}{\partial t} = \frac{1}{A} \frac{\partial}{\partial s} \left(A\kappa \frac{\partial T}{\partial s} \right) - \frac{\kappa}{T} \left(\frac{\partial T}{\partial s} \right)^2 \quad . \tag{2.11}$$

We use the Spitzer (1962) formula for thermal conductivity,

$$\kappa = \alpha T^{5/2} \tag{2.12}$$

where, with sufficient accuracy for our purposes, we may take $\alpha = 10^{-6}$.

Equation (2.11) is nonlinear, but it is amenable to solution by separation of variables. We assume that T is of the form

$$T(s,t) = T_M \theta(t) \varphi(s) \quad . \tag{2.13}$$

For convenience, we choose

$$\theta(0) = 1 \ , \quad \varphi(0) = 1 \quad , \tag{2.14}$$

so that T_M is the maximum temperature of the plasma (the initial temperature at the top of the loop). We may substitute (2.13) into equation (2.11) and obtain

$$- \frac{5}{2} \frac{p}{\alpha T_M^{7/2}} \frac{d}{dt} \left(\theta^{-7/2}\right) = \frac{1}{A} \frac{d}{ds} \left(A \frac{d\psi}{ds}\right) - \frac{2}{7} \frac{1}{\psi} \left(\frac{d\psi}{ds}\right)^2 \quad , \tag{2.15}$$

where $\psi(s)$ is related to $\varphi(s)$ by

$$\psi = \varphi^{7/2} \quad . \tag{2.16}$$

In equation (2.15), the variables are separated so that we may set each side equal to $-k^2$ (independent of both t and s). The equation for $\theta(t)$,

$$\frac{d}{dt} \left(\theta^{-7/2}\right) = \frac{2}{5} \frac{\alpha T_M^{7/2}}{p} k^2 \quad , \tag{2.17}$$

may be integrated to give

$$\theta(t) = (1 + t/\tau_c)^{-2/7} \quad , \tag{2.18}$$

where

$$\tau_c = \frac{5p}{2\alpha T_M^{7/2} k^2} \quad . \tag{2.19}$$

The equation for ψ becomes

$$\frac{d^2\psi}{ds^2} - \frac{2}{7} \frac{1}{\psi} \left(\frac{d\psi}{ds}\right)^2 + \frac{1}{A} \frac{dA}{ds} \frac{d\psi}{ds} = - k^2 \quad . \tag{2.20}$$

We see from equation (2.14) and the symmetry of the flare loop that we require that

$$\psi = 1, \quad \frac{d\psi}{ds} = 0 \text{ at } s = 0 \quad . \tag{2.21}$$

However, if s_b is the value of s at the "base" of the model (i.e., at the chromosphere), the temperature must drop to the low chromospheric value at s_b. For our purposes, it is convenient to set

$$\psi(s_b) = 0 \quad . \tag{2.22}$$

The position of the chromosphere will actually be not at the point where $\psi = 0$ (i.e. $T = 0$), but where $T \approx 10^4$ K, but this difference is small compared with the size of typical flare loops. The conditions (2.21) and (2.22) can be met only for a unique value of k in equation (2.20). This value will of course depend implicitly also on the area function A(s). For either type of magnetic-field tube (that produced by a point dipole or that produced by a line dipole), we shall wish to consider a range of values of s_b. Rather than prescribe s_b and then determine k as an eigenvalue of the differential equation (2.20), it is clearly simpler to consider a range of values of k and determine s_b for each value. This may be done by finding a solution of the equation with the initial conditions (2.21), and then finding the point s_b at which $\psi = 0$.

III. Results

(a) Temperature Profile

For the case of a loop of constant cross-section, equation (2.20) can be integrated directly yielding:

$$\frac{\varphi}{2}\sqrt{1-\varphi^{3/2}} - \frac{2\sqrt{1-\varphi^{3/2}}}{\sqrt{3}+1-\sqrt{\varphi}} - \frac{(\sqrt{3}-1)}{3^{1/4}}\,F\left(\beta(\varphi),\ \sin 75^{o}\right) \tag{3.1}$$

$$+\ 2.3^{1/4}\,E\left(\beta(\varphi),\ \sin 75^{o}\right) = \frac{1}{2}\sqrt{\frac{7}{6}}\,ks \quad ,$$

where

$$\beta(\varphi) = \arccos\left[\frac{\sqrt{3}-1+\sqrt{\varphi}}{\sqrt{3}+1-\sqrt{\varphi}}\right] \tag{3.2}$$

and F and E are the elliptic integrals of the first and second kind respectively. The constant k can now be expressed in terms of the position s_b of the base. Using equations (3.1) and (3.2), we find that for the planar case,

$$k = 1.60/s_b \quad . \tag{3.3}$$

For loops of variable cross-section, equation (2.20) has been integrated numerically. The important parameters that characterize the geometry are the loop length s_b and the ratio of the cross-sectional area $A(0)$ at the top of the loop to the area $A(s_b)$ at the base. We term this ratio the "compression factor" Γ:

$$\Gamma = A(0)/A(s_b) = B(s_b)/B(0) \quad . \tag{3.4}$$

Rust and Bar (1973) find that $\Gamma \leq 30$ in the flare of August 7, 1972.

For a given form of A(s), we may solve equation (2.20) for $\varpi(s)$. In Figure 3.1 we plot the temperature scale height H implied by our model,

$$H(T) = \left| \frac{1}{T} \frac{dT}{ds} \right|^{-1} , \qquad (3.5)$$

as a function of temperature along the loop. This is done for the case of a constant-area loop and for a flux tube due to a line-dipole source with a compression factor $\Gamma = 30$. The results for a point-dipole source are almost identical to those of a line-dipole. The fact that the scale height H becomes infinite at the top of the loop simply reflects the fact that the spatial derivative of the temperature is zero at the top of the loop. This peculiarity is without physical significance; it simply means that the spatial variation of temperature is determined by the second derivative of the temperature rather than the first derivative.

The true size scale over which T varies is, of course, less than the loop length. For $T < 10^{-1}$, the scale height is small compared to the loop length, $H(T) < 10^{-2} s_b$, and decreases as $T^{5/2}$ in both the constant-area and the variable-area cases. The loop would therefore appear to an observer to be almost isothermal with a very thin transition region, as is the case for the quiet corona.

For comparison we also plot in Figure 3.1 the temperature scale height given by the static model discussed by Antiochos and Sturrock (1976). From this figure we find that at low temperatures ($T < 10^{-1}$) the temperature profile is given by: $T \propto s^{2/5}$ for evaporative cooling, and $T \propto s^{2/7}$ for static cooling. Hence the heat flux F is linearly

proportional to T in the evaporative models, whereas F ~ const. in the static models. This result argues strongly in favor of the evaporative models.

For temperatures and size scales typical of flares, the heat flux into the chromosphere implied by the static models is very large, in excess of 10^8 ergs cm^{-2} s^{-1}. It is difficult for static models to account for the dissipation of such a large flux; however, in our present model this flux is reduced by the evaporation process. The heat flux into the chromosphere is approximately three orders of magnitude lower for an evaporative model than for a static model.

(b) Cooling Time Scale

We can evaluate the cooling time τ_c in equation (2.18) by using equation (3.3). For typical loop parameters,

$$T \sim 10^7 \text{ K}, \quad n \sim 10^{10.5} \text{ cm}^{-3} \quad \text{and} \quad s_b \sim 10^{9.5} \text{ cm} , \tag{3.6}$$

equations (2.19) and (3.3) yield

$$\tau_c \approx 10^2 \text{ sec.} \tag{3.7}$$

The radiative cooling time is given by

$$\tau_R \approx \frac{3}{2} \frac{p}{n^2 \Lambda(T)} , \tag{3.8}$$

where $\Lambda(T)$ has been computed by Raymond et al. (1976). For the above parameters (3.6), we find that $\tau_R \approx 10^3$ sec; hence, our assumption that conduction dominates the cooling is justified. However, as the temperature decreases the ratio τ_c/τ_R increases until eventually radiation dominates and evaporation becomes unimportant. For the loop described above, we expect this to occur at $T \leq 5 \times 10^6$ K.

We have also calculated the cooling times for loops due to either a point dipole or line dipole source. The effect of the geometry is shown in Figure 3.2, where we plot the ratio of the cooling times for a loop and for a planar (constant cross-section) model as a function of Γ. As in the static case (Antiochos and Sturrock, 1976), the effect of the compression factor is to increase the cooling time; however, we still expect that conduction dominates over radiation during the initial stages if $T \geq 10^7$ K.

The other main assumption in our model is that the evaporation velocities are small compared to the speed of sound. For the planar case, the Mach number can be obtained directly from equations (2.9) and (3.1):

$$M = \frac{v}{c} = 10^{-10.6} \frac{T_M^3}{ps_b} \varphi^{1/2} (1 - \varphi^{3/2})^{1/2} (1 + \frac{t}{\tau_c})^{-6/7} \qquad (3.9)$$

The maximum value of M occurs at $t = 0$ and $\varphi = (2/5)^{2/3} \approx .5$. For the parameters in (3.6), we find that $M \leq 10^{-1}$, so that our assumption is valid. From the form of the time-dependence of M and T, we find that $M \propto T^3$ for fixed s, hence our approximation improves as the loop cools.

(c) Radiation

Various authors have attempted to calculate the emission measure and the temperature of flare regions from soft x-ray observations (e.g. Kahler et al., 1970; Horan, 1971). Craig and Brown (1976) point out that these calculations are inherently inaccurate, and suggest that one should instead assume a definite model for the structure of a flare region and then test this model by comparing the expected radiation with observations. We, therefore, calculate the

evolution of the soft x-ray emission predicted by our evaporative loop model.

Generally, the observations consist of measurement of the total flux of x-rays in some energy range. Hence we must compute

$$\mathcal{F}(E_1, E_2, t) = \int_{E_1}^{E_2} dE \int_V d^3x \; \eta(E, x, t) \quad , \tag{3.10}$$

where the spatial integration is over the volume of the loop and η is the energy flux at the earth from a unit volume of plasma. If the dominant radiation process is bremsstrahlung, the emissivity η(keV cm^{-3} s^{-1} keV^{-1}) is given by

$$\eta = a e^{-E/kT} n^2 T^{-1/2} \quad , \tag{3.11}$$

where $a = 10^{-38.09}$ for T in ^oK, (Kahler et al., 1970). Using equations (3.1) and (3.11) and integrating equation (3.10) over E, we obtain for a loop of constant cross-section A:

$$\mathcal{F}(r_1, r_2, t) = C_1 \, \theta^{-3/2}(t) \int_0^1 d\varphi \, \frac{e^{-\frac{r_1}{\theta\varphi}} - e^{-\frac{r_2}{\theta\varphi}}}{\sqrt{1 - \varphi^3}^{3/2}} \quad , \tag{3.12}$$

where

$$C_1 = 10^{-13.8} \frac{p^2 A s_b}{T_M^{3/2}} \tag{3.13}$$

and

$$r_1 = \frac{E_1}{kT_M} \; , \quad r_2 = \frac{E_2}{kT_M} \quad . \tag{3.14}$$

In Figure 3.3 we plot L for the particular values $r_1 = 1/2$ and $r_2 = 1$ as a function of t/τ_c. Assuming a maximum loop temperature

$T_M = 2 \times 10^7$ K, these values for r_1 and r_2 correspond to a soft x-ray range from 1 - 2 keV. We also plot the time dependence of the temperature and of the emission measure in Figure 3.3. Note that even though the temperature is continuously decreasing, $\mathcal{L}$ increases initially due to the increasing emission measure and has a maximum at $t/\tau_c = 50$. For larger values of r_1 and r_2, e.g. $r_1 = 2$ ($E_1 = 4$ keV) and $r_2 = 4$ ($E_2 = 8$ keV), the exponential term in the emissivity (3.11) dominates, and L decreases monotonically. We find that these results are insensitive to the compression factor Γ because the x-ray emission comes mainly from the high-temperature material high in the loop.

The qualitative features of Figure 3.3 are in agreement with soft x-ray observations. However, we would not expect to find detailed agreement, since we have calculated the emission from only a single loop, whereas a flare is likely to consist of many loops at different stages in their evolution. In addition, we have neglected any heating which may be present during the decay phase of flares. However, our results do predict a rise in soft x-ray flux concurrent with a decrease in temperature, whereas in the static models the emission must decrease with the temperature.

We believe that a strong observational test of our model may lie in the spectrum of the radiation. From the form of the scale height, Figure 3.1, we note that an evaporative loop contains relatively more plasma at low temperatures ($\leq 10^6$ K) than does a static one, which implies that the spectra of the emitted radiation (especially at EUV wavelengths) should be significantly different in the two cases. This is clearly illustrated in Figure 3.4 where we plot, for both models,

the total radiative losses $\epsilon(T)$ due to plasma at different temperatures along the loop, i.e.

$$\epsilon(T) = n^2 \Lambda(T)\, H(T) \quad , \tag{3.15}$$

where we use Cox and Tucker's (1969) values for $\Lambda(T)$, and H and n are in units of loop length s_b, and density at the top of the loop $n(s = 0)$, respectively. The temperature at the top of the loop is assumed to be, $T_M = 10^7$ K. We note that in the static case the highest temperature plasma is responsible for most of the energy loss whereas, in the evaporative loop, plasma at $\sim 5 \times 10^5$ K radiates most strongly. In a later paper we intend to calculate the spectra for both models in detail, in particular the emission in various EUV and x-ray lines, and to compare these calculations with recent Skylab observations.

Acknowledgements

One of us (P.A.S.) wishes to thank Professors G.R. Burbidge and L.E. Peterson and their colleagues at the University of California at San Diego for their kind hospitality in the spring of 1975, when this work was initiated. This work was supported by the National Aeronautics and Space Administration under grant NGL 05-020-272 and the Office of Naval Research under contract N00014-75-C-0673.

References

Antiochos, S.K. and Sturrock, P.A. 1976, Sol. Phys. (in press).

Cox, D.P. and Tucker, W.H. 1969, Ap. J. 157, 1157.

Craig, I.J.D. and Brown, J.C. 1976, Astron. and Astrophys. 49, 239.

Horan, D.M. 1971, Sol. Phys. 21, 188.

Hudson, H.S. and Okhi, K. 1972, Sol. Phys. 23, 155.

Jefferies, J.T. and Orrall, F.Q. 1965, Ap. J. 141, 519.

Kahler, S.W., Meekins, J.F. and Kreplin, R.W. 1970, Ap. J. 162, 293.

Neupert, W.M. 1968, Ap. J. Letters 153, L59.

Phillips, K.J.H. and Neupert, W.M. 1973, Sol. Phys. 32, 209.

Raymond, J.C., Cox, D.P. and Smith, B.W. 1976, Ap. J. 204, 290.

Rust, D.M. and Bar, V. 1973, Sol. Phys. 33, 445.

Spitzer, L. 1962, "Physics of Fully Ionized Gases", (Wiley Interscience, New York), Ch. 5.

Strauss, F.M. and Papagiannis, M.D. 1971, Ap. J. 164, 369.

Sturrock, P.A. 1973, Proc Symp. on High Energy Phenomena on the Sun, Greenbelt, Maryland.

Zaumen, W.T. and Acton, L.W. 1974, Sol. Phys 30, 139.

Figure Captions

Figure 3.1: The temperature scale height as a function of temperature along the loop for three models. The top solid line refers to an evaporative model of constant cross-section. The broken line refers to an evaporative model for a loop due to a line-dipole source with $\Gamma = 30$. The bottom solid line refers to a static model of constant cross-section.

Figure 3.2: Ratio of cooling times for a variable cross-section model as a function of Γ. The solid line refers to a loop due to a point-dipole source and the broken line to a loop due to a line-dipole source.

Figure 3.3: The evolution of the soft x-ray emission $\mathcal{E}$ between 1 - 2 keV, the temperature T, and the emission measure (E.M.) for a loop of initial temperature, $T_M = 2 \times 10^7$ K.

Figure 3.4: The radiative losses per unit logarithmic temperature interval of plasma in a loop as a function of temperature along the loop. The top line refers to an evaporative model and the bottom line refers to a static model.

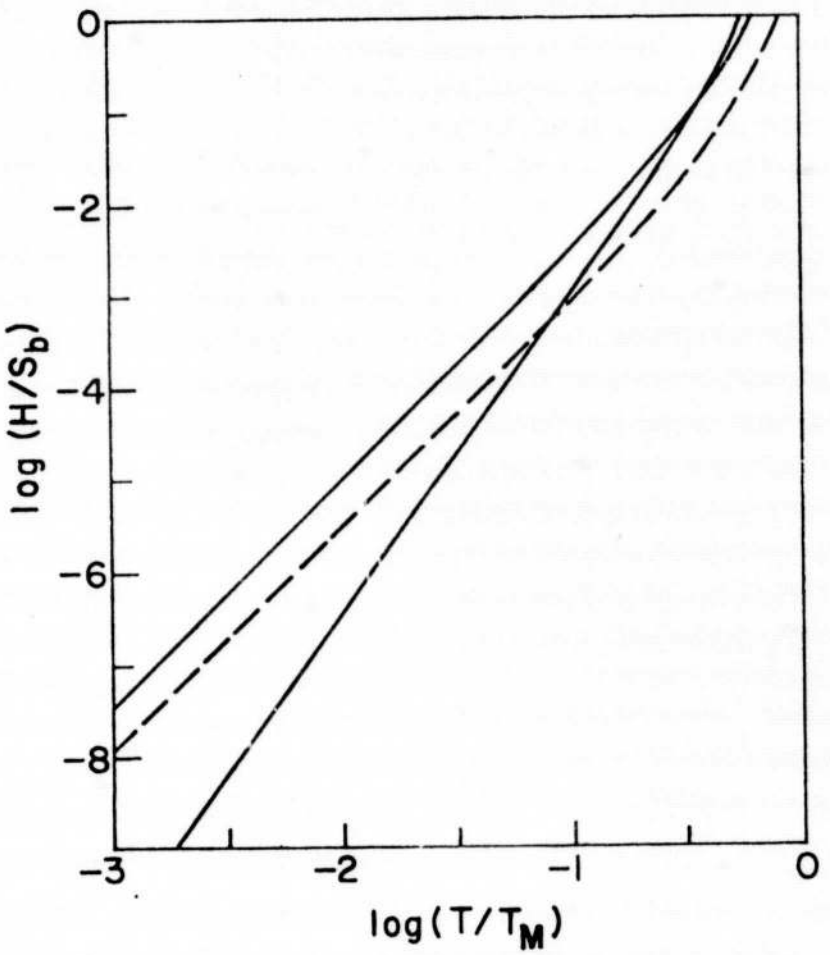

Figure 3.1

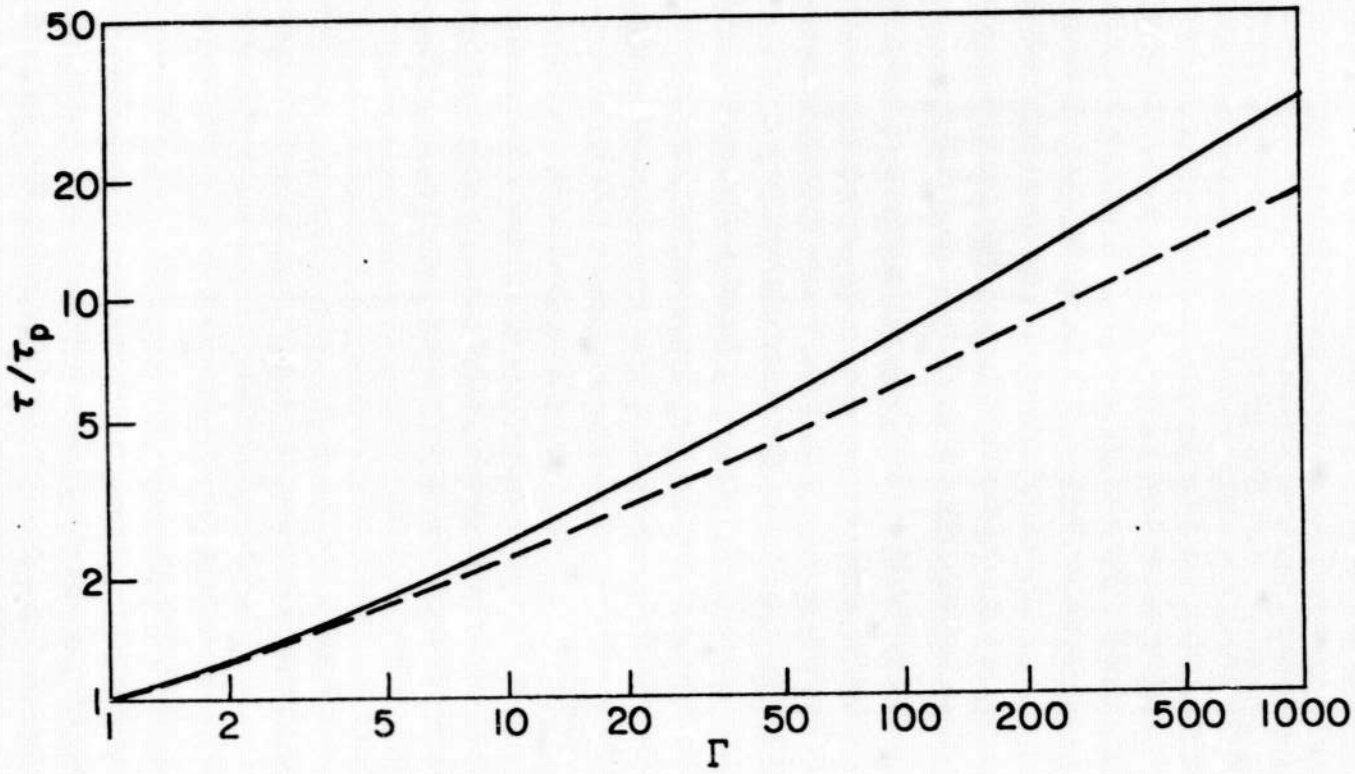

Figure 3.2

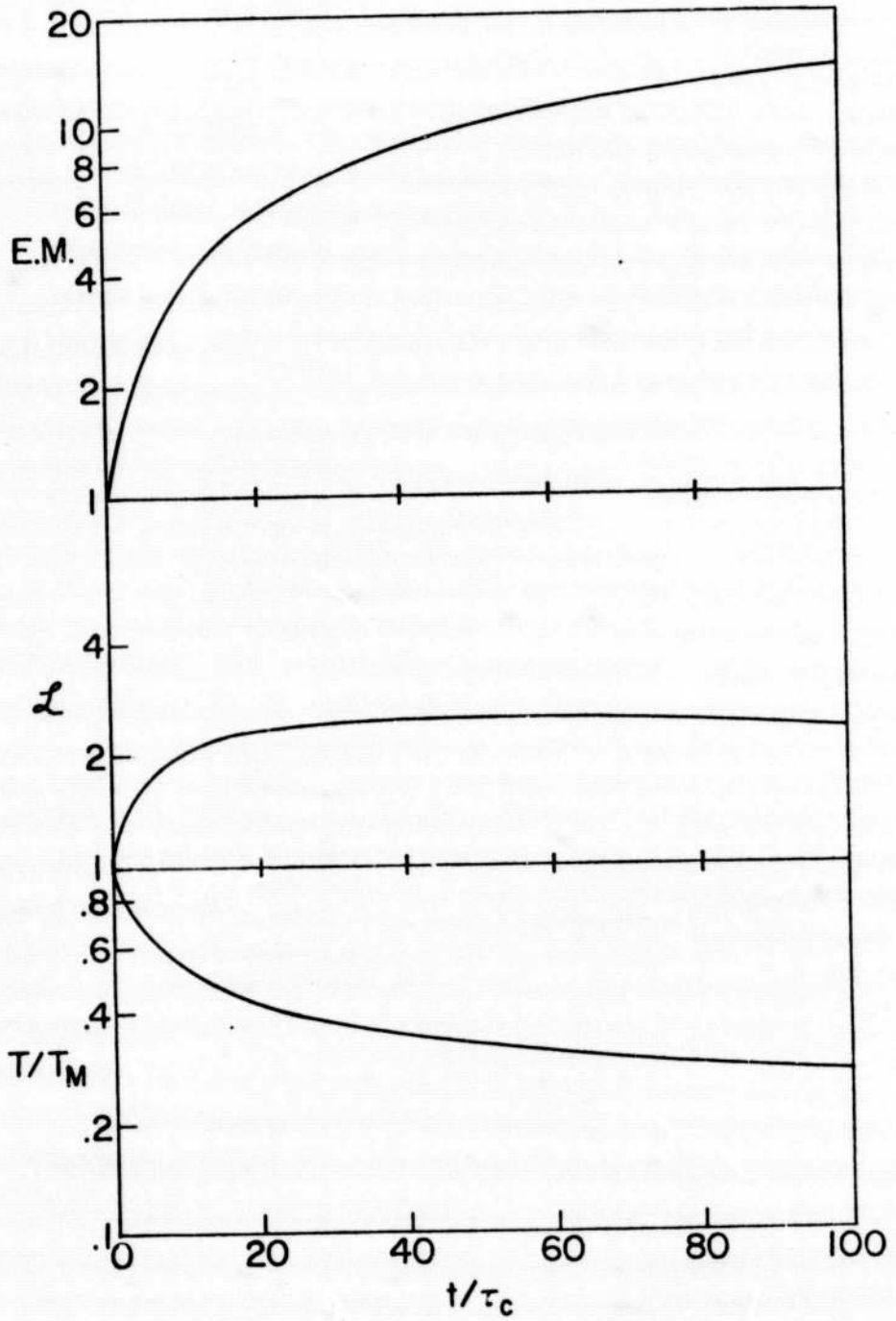

Figure 3.3

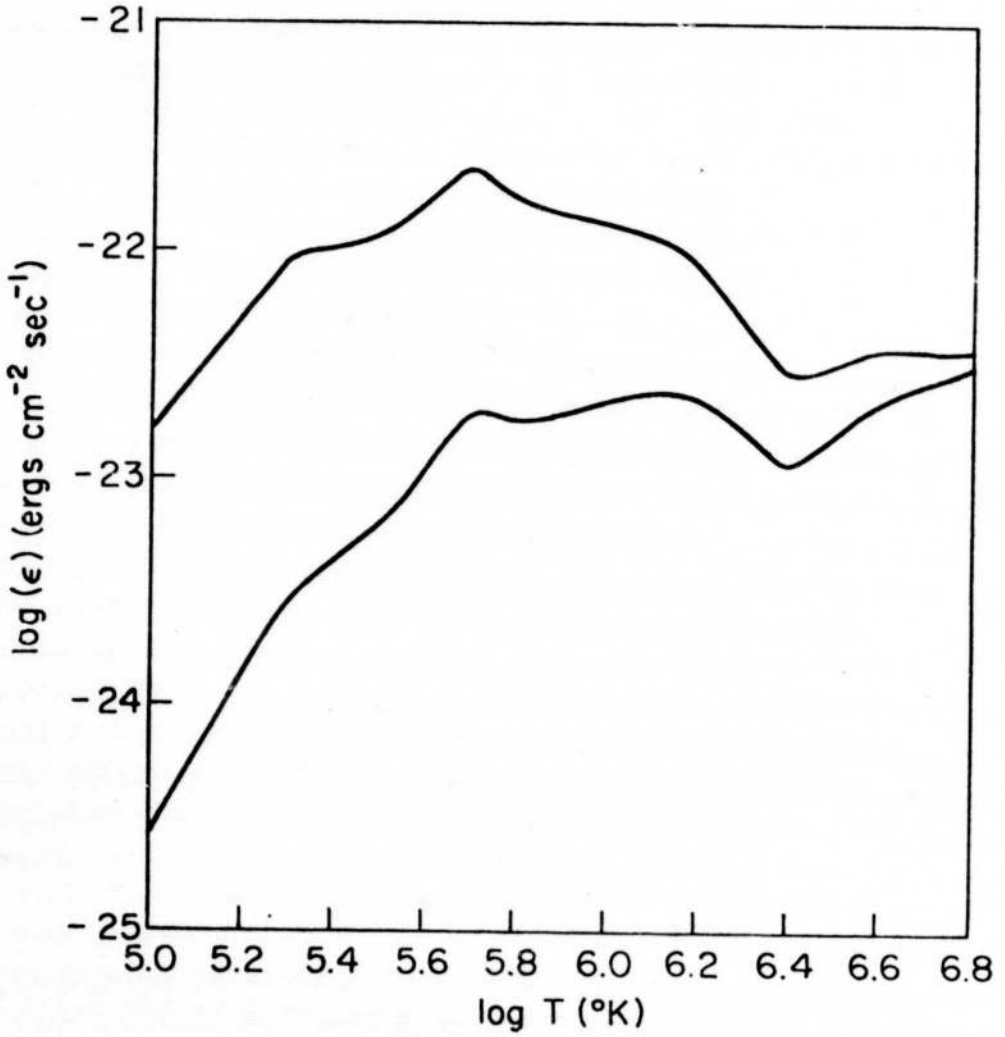

Figure 3.4